Supramolecular Chemistry
Publication details, including instructions for authors and subscription information:
http://www.informaworld.com/smpp/title~content=t713649759

Novel Attempts to Change the Colour of Dye Molecules Utilizing the Aggregation Mode of Saccharides

Masato Amaike[a]; Hideki Kobayashi[a]; Kazuo Sakurai[a]; Seiji Shinkai[a]
[a] Chemotransfiguration Project, Japan Science and Technology Corporation (JST), Kurume, Fukuoka, Japan

Online publication date: 29 October 2010

To cite this Article Amaike, Masato , Kobayashi, Hideki , Sakurai, Kazuo and Shinkai, Seiji(2002) 'Novel Attempts to Change the Colour of Dye Molecules Utilizing the Aggregation Mode of Saccharides', Supramolecular Chemistry, 14: 2, 245 — 253
To link to this Article: DOI: 10.1080/10610270290026158
URL: http://dx.doi.org/10.1080/10610270290026158

Supramolecular Chemistry, 2002 Vol. 14 (2-3), pp. 245–253

Taylor & Francis
Taylor & Francis Group

Novel Attempts to Change the Colour of Dye Molecules Utilizing the Aggregation Mode of Saccharides

MASATO AMAIKE, HIDEKI KOBAYASHI, KAZUO SAKURAI and SEIJI SHINKAI*

Chemotransfiguration Project, Japan Science and Technology Corporation (JST), 2432 Aikawa, Kurume, Fukuoka 839-0861, Japan

(Received 24 August 2001)

Ten saccharide-dye (azophenol and azonaphthol) conjugate molecules and four methylated reference compounds were synthesized. The purpose of the present study using these molecules is to change the colour of the common dye moiety, both in solution and in solid by the structural difference in the saccharide moieties and eventually to mimic the colour creation mechanism in a nature's flower family. In azophenol derivatives, the solution (THF) colour was more or less the same but the solid colour was significantly different (yellow–orange–pink). The XRD study established that the colour change is correlated to the crystallinity of the solid samples: the λ_{max} shifts to shorter wavelength with the increase in the crystallinity. In azonaphthol derivatives, the solution colour was more different than the solid colour. The spectroscopic studies established that this change is due to an azo-hydrazone tautomerism. The colour changes were quantitatively expressed by the CIE *L*a*b colourimetric system. The foregoing results indicate that the colour of the dye molecules can be changed utilizing the intra- and intermolecular hydrogen-bonding interactions among the appended saccharide moieties.**

Keywords: Aggregation mode; Saccharide; Azo-hydrazone tautomerism; Colour change; Crystallinity

INTRODUCTION

The survey of the past literatures on the chemistry of flowers teaches us that an anthocyanin dye family is used in most flowers and the subtle change in the colour tone is controlled by the intermolecular and/or intramolecular interactions of saccharides covalently bound to the anthocyanin dye [1–3]. The purpose of the present research is to reproduce such a saccharide-induced colour change of dye molecules in a totally artificial system. Recently, it was shown that boronic acids serve as an efficient "covalent-bond-forming interface" for saccharides [4–12]. Thus, we previously synthesized a few boronic acid-appended dye molecules (e.g. **1**) and evaluated if the solution colour can be changed by saccharide, covalently-bound to the boronic acid site [13–19]. It was shown that the colour change is in fact induced by the sugar-binding event related to (i) a change in neutral sp^2 boron to anionic sp^3 boronate, (ii) a shift of association–dissociation equilibria and (ii) a synergistic effect of (i) and (ii) [13–16], but the mechanistic view including the boronic acid–saccharide interactions was fairly complicated [14,15]. In the present study, we aimed at inducing the colour change of dye molecules by a more straightforward method mimicking the nature's palette: that is, according to a concept of combinatorial chemistry various saccharide–dye conjugates were synthesized utilizing a saccharide library as building blocks and their colours were evaluated in the solution state as well as in the solid state. We have found that the colour is slightly changed in the solution state where the aggregation occurs under various association–dissociation equilibria, but largely changed in the solid state where the molecular

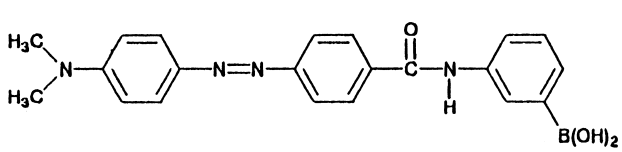

1

*Corresponding author.

ISSN 1061-0278 print/ISSN 1029-0478 online © 2002 Taylor & Francis Ltd
DOI: 10.1080/10610270290026158

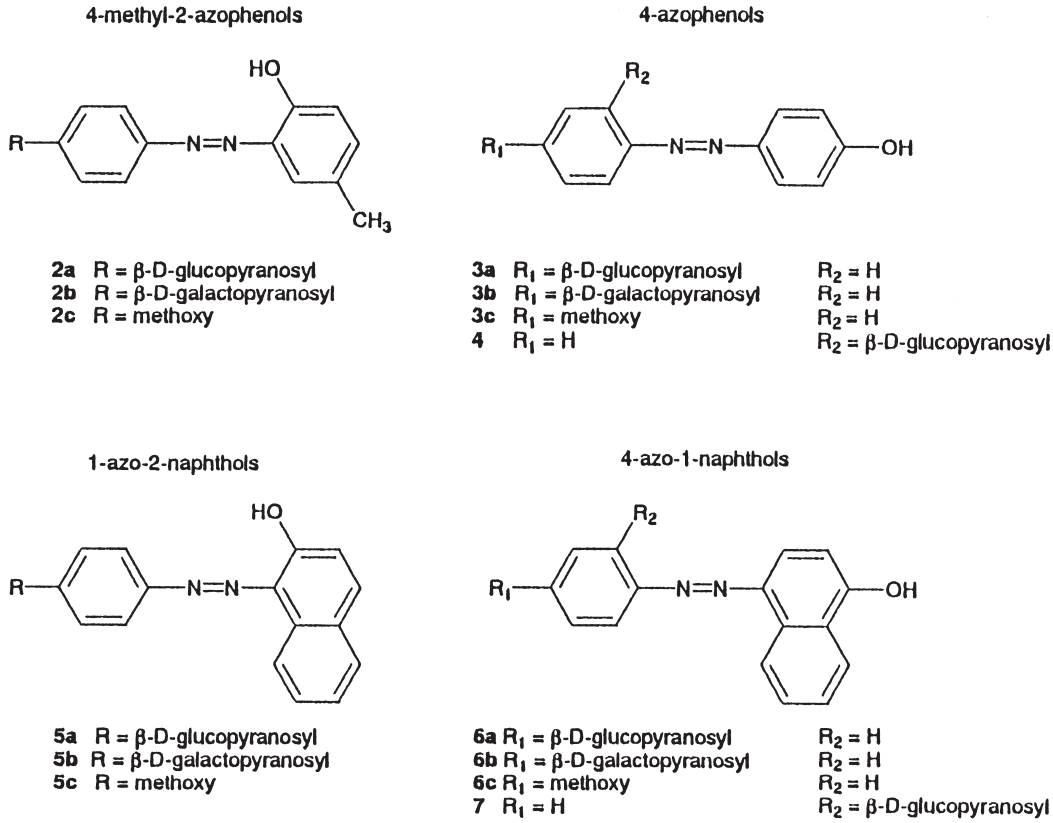

SCHEME 1 Saccharide-dye conjugates

packing is directly affected by the absolute configuration of the saccharide moiety.

RESULTS AND DISCUSSION

In the process of molecular design of saccharide–dye conjugate molecules (see Scheme 1), the following factors were taken into consideration. Firstly, the dye moiety is a 4-methyl-2-azophenol (**2a**–**2c**), 4-azophenol (**3a**–**3c**, and 4), 1-azo-2-naphthol (**5a**–**5c**) or 4-azo-1-naphthol (**6a**–**6c**, and **7**) group whereas the saccharide moiety is a β-D-glucopyranosyl or β-D-galactopyranosyl group. One may thus estimate the influence of the saccharide structure on the colour of the aggregated or solid dye molecules. Secondly, one can expect a change in the azo-hydrazone tautomerism for these azophenol and azonaphthol skeletons. Since this tautomerism is sensitive to the polarity of the solvent, the saccharide-induced slight change in the aggregation mode may be reflected by a shift of this tautomerism and induce a colour change. Thirdly, the methyl derivatives (**2c**, **3c**, **5c**, and **6c**) are used as reference compounds without the saccharide group.

Figure 1 shows the absorption spectra of **2a**, **2b**, and **2c** bearing a 4-methyl-2-azophenol chromophoric group. It is seen from Fig. 1B that their absorption spectra in solution are more or less the same. In the solid state, on the other hand, the absorption spectra are significantly different (Fig. 1A): in particular, **2a** and **2c** have a weak absorption tail in longer wavelength region (>550 nm). However, the colour (orange yellow) is visually not so different, although **2a** and **2c** are a little more reddish than **2b** (Fig. 2A).

Figure 3 shows the absorption spectra of **3a**, **3b**, **3c**, and **4** bearing a 4-azophenol chromophoric group. Again, the spectral difference was not observed in THF (Fig. 3B). On the other hand, the colour is apparently different in the solid state (Fig. 2B): **3a** and **3c** are orange yellow whereas **3b** is pink and **4** is orange. Examination of the absorption spectra (Fig. 3A) reveals that the λ_{max} values for **3a**, **3b**, and **3c** (314,317 and 316 nm, respectively) in the solid state appear at shorter wavelength than those in THF (ca.358 ± 1 nm). In contrast, the λ_{max} for **4** is scarcely changed between THF (360 nm) and solid (365 nm). The results suggest that in the solid state, some dipole–dipole interaction arising from the molecular packing exists in **3a**, **3b**, and **3c** whereas the 4-azophenol moiety in **4** is insulated from each other even in the solid state to behave like a "monomer" in solution. To obtain evidence for this rationale, we measured powder XRD spectra for solid **3a**–**3c**, and **4** samples (Fig. 4). It is seen from Fig. 4 that all samples result in a strong peak at around $2\theta = 22°$. **3c**, a reference compound with a methyl group is a good crystal. Although **3a** and **3b**

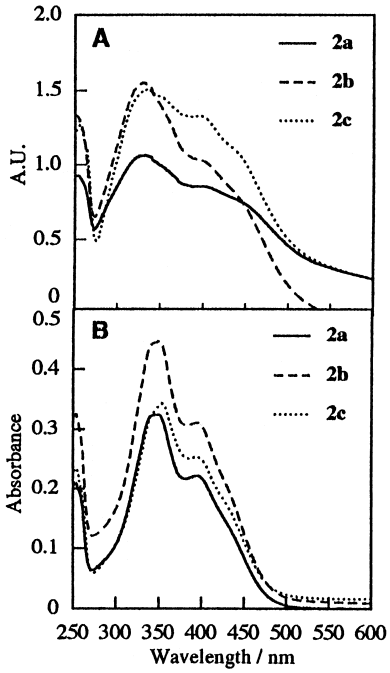

FIGURE 1 Absorption spectra of **2a**, **2b**, and **2c** (A) in solid (recrystallized from THF) and (B) in THF (2.00×10^{-5} mol dm^{-3}).

are not so good crystals as **3c**, they are basically classified into crystals. On the other hand, **4** is classified into amorphous powder from its broad peaks. The findings support the view that only the 4-azophenol moieties in solid **4** are not stacked regularly with each other but rather exists discretely, giving the absorption spectrum similar to that in THF. One can thus regard that the difference in the molecular packing, which is affected by the covalently-linked saccharide moiety, is reflected by the colour of the solid samples.

To obtain a more quantitative insight into the colour difference in the solid state, we applied a CIE $L^*a^*b^*$ colourimetric system. Among the colour specifications proposed, the $L^*a^*b^*$ system is most popular. It was standardized by the CIE in 1976 and has been adopted in various fields of industry [20]. In this trichromatic $L^*a^*b^*$ system, L^* represents lightness whereas a^* and b^* represent chromaticity. Thus, the image of the colour space is represented by an orthogonal coordinate. The measured a^* and b^* values were corrected for the blank. The results are summarized in Table I together with other spectroscopic parameters.

Plots of a^* *vs.* b^* for **2a**–**3a**, and **4** are shown in Fig. 5, where $+a^*$, $-a^*$, $+b^*$ and $-b^*$ values correspond to red, green, yellow and blue axes, respectively. **2a** and **2c** having an absorption tail in longer wavelength region features a^* larger than **2b**, indicating that they are more reddish. The b^* values for **2b** and **2c** are similar to each other but larger than that of **2a**. Therefore, it is clear that the β-D-glucopyranosyl group and the β-D-galactopyranosyl

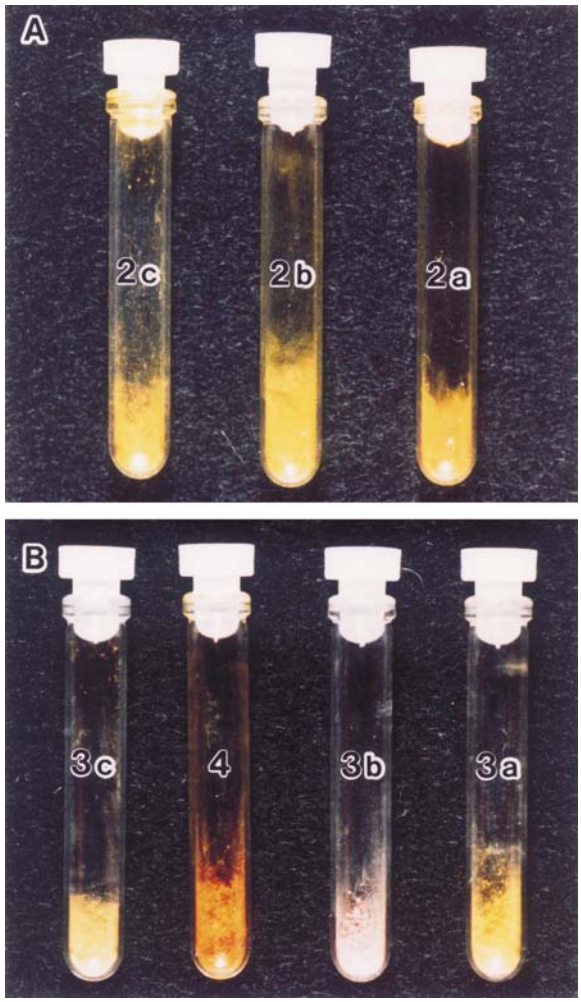

FIGURE 2 Photographs of **2a**–**2c** (A: upper) and **3a**–**3c**, and **4** (B: lower): the solid samples were all recrystallized from THF.

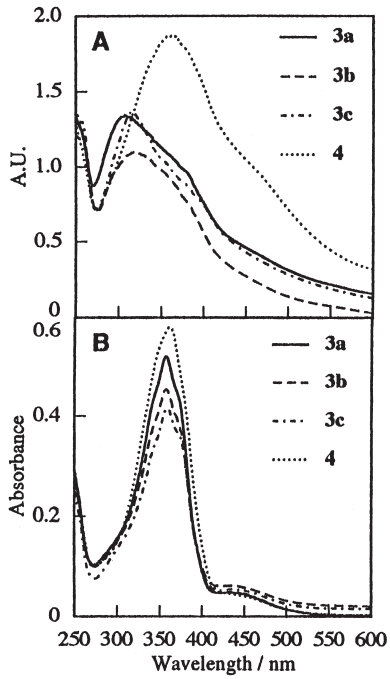

FIGURE 3 Absorption spectra of **3a**, **3b**, **3c**, and **4** (A) in solid (recrystallized from THF) and (B) in THF (2.00×10^{-5} mol dm^{-3}).

TABLE I Colour **2a-4**

	Colour	Solid state (crystallized from THF) λmax/nm[a]	Colour analysis[c] L*	a*	b*	Solution state (in THF) λmax/nm[b]
2a	orange-yellow	335, 403	42.4	28.8	47.7	350, 397
2b	orange-yellow	332, 394	65.9	19.9	77.1	350, 394
2c	orange-yellow	334, 397	65.4	28.5	72.2	353, 394
3a	orange-yellow	314	79.1	16.3	70.9	357
3b	pink	317	76.6	28.3	28.6	358
3c	orange-yellow	316	58.0	4.7	37.4	359
4	orange	365	58.2	41.4	69.9	360

[a] Measured by a KBr pellet method. [b] 5×10^{-5} mol dm^{-3} and 1 = 1 cm. [c] Colour analyses were performed according to the CIE L *a *b *colourimetric system. The values are averaged after three measurements.

group can influence the molecular packing of the chromophoric group differently. Plots of **3a**–**3c**, and **4** are scattered on the a^*–b^* coordinate. **3a** and **4** bearing the same β-D-glucopyranosyl group at the different position give the similar b^* values, whereas **3b** bearing β-D-galactopyranosyl group gives the b^* value much smaller than **3a**. The results imply that the difference in the saccharide structure is mainly reflected by the b^* value.

It is known that in an azo-hydrazone tautomerism the λ_{max} for hydrazone form appears at the longer wavelength (around 500 nm) [21–24]. For **2a**–**2c**, **3a**–**3c**, and **4**, however, such a peak ascribable to the hydrazone form was not observed both in THF and the solid state. In IR spectroscopy (KBr disk), the $\nu_{C=O}$ band arising from the hydrazone form did not appear. These results consistently indicate that in azophenol derivatives the azo form is much more stable than the hydrazone form. To shift this tautomerism to the hydrazone form, we newly designed **5a**–**5c**, **6a**–**6c**, and **7** bearing an azo-naphthol skeleton. As expected, the $\nu_{C=O}$ band was clearly detected in the IR spectra (KBr disk) of **5a**–**5c**, **6a**–**6c**, and **7** at 1610–1648 cm^{-1}, indicating that these azonaphthol derivatives are rendered to the azo-hydrazone tautomerism. One can thus expect a colour change arising from the shift of this tautomerism for these dye molecules.

Absorption spectra of **5a**–**5c** are shown in Fig. 6. In THF, their absorption spectra are more or less similar to each other and give the λ_{max} at around 420 nm, indicating that they mostly exist in the azo form (Fig. 6B). This implies that in THF the saccharide–saccharide interaction is not so significant as to affect the electronic transition band of the azo-2-naphthol group. In the solid state (KBr disk), they give the $\nu_{C=O}$ band at 1619 cm^{-1} ascribable to the hydrazone form. As expected, the adsorption spectra are significantly different (Fig. 6A): in particular, **5c** without the saccharide substituent has the strong hydrazone band at 565 nm. It is known that the azo form is more stabilized in polar, protic solvents owing to the efficient hydrogen-bonding interaction between the OH group and solvent molecules [21–24]. In the present system, the OH group interacts with saccharide OH groups to stabilize the azo form.

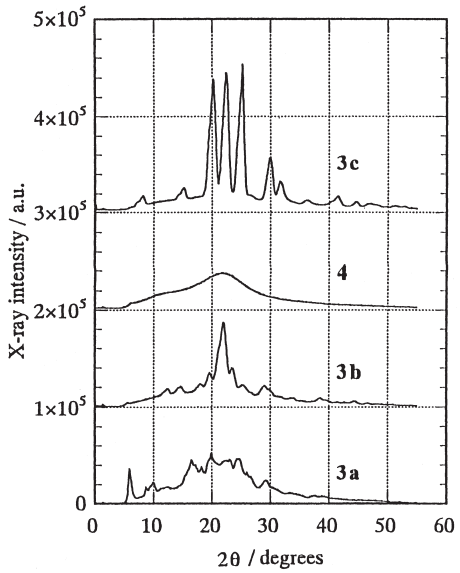

FIGURE 4 Powder XRD patterns for **3a**, **3b**, **3c**, and **4**.

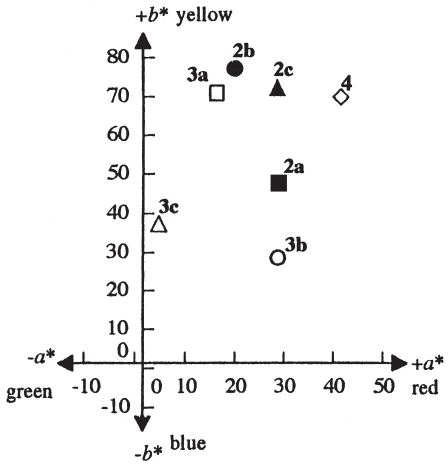

FIGURE 5 a^*–b^* plots for **2a**–**3c**, and **4**.

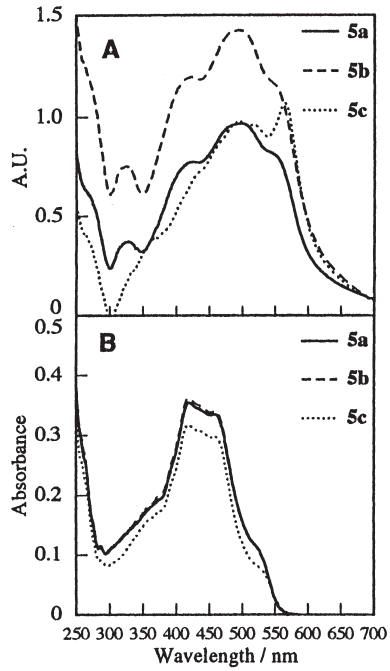

FIGURE 6 Absorption spectra of **5a**, **5b**, and **5c** (A) in solid (recrystallized from THF) and (B) in THF (2.00×10^{-5} mol dm^{-3}).

The picture of these solid samples is shown in Fig. 7A: the red colour of **5c** is somewhat deeper than that of **5a** and **5b**, but the visual difference is not so clear as we expected.

Absorption spectra of **6a**–**6c**, and **7** bearing the 4-azophenyl-1-naphthol group are shown in Fig. 8. In THF, the absorption spectra of **6a**–**6c** bearing the saccharide substituent at the 4′-phenyl position have the λ_{max} at around 400 nm, indicating that they mostly exist in the azo form. In contrast, **7** bearing the saccharide substituent at the 2′-phenyl position has the strong $\nu_{C=O}$ band at 1648 cm^{-1} in the IR spectrum (in THF) and gives the λ_{max} at around 461 nm. The results show that **7** predominantly exists in the hydrazone form. This tautomerism shift is attributed to the formation of an intramolecular hydrogen-bond between the 1-*O* in the 2′-saccharide substituent and the NH in the hydrazone form (Fig. 9). Absorption spectra measured in the solid state are shown in Fig. 8A. Judging from the colour change, the major species for **7** is the hydrazone form and that for **6a** and **6b** is the azo form. On the other hand, **6c** gives rise to a new absorption band at 480 nm assignable to the hydrazone form. As expected, the solid colour of **6c** is brown and very different from the red colour of **6a**, **6b**, and **7**.

Powder XRD spectra were measured for **6a**–**6c**, and **7** (Fig. 10). **6a** and **6b** give the similar XRD patterns with a strong peak at $2\theta = 22°$, like those in Fig. 4. The XRD patterns for **6c** and **7** are different from those: judging from the sharp peaks, **6c** should have the crystal-like nature. Since the colour of **6c** is

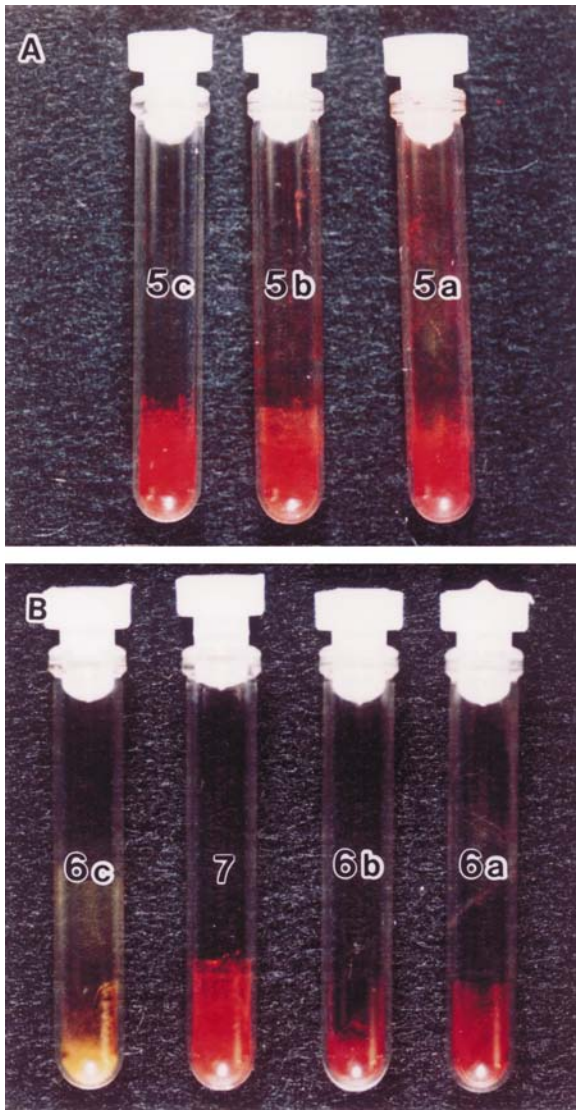

FIGURE 7 Photographs of **5a**–**5c** (A: upper) and **6a**–**6c**, and **7** (B: lower): the solid samples were all recrystallized from THF.

largely different, one can again propose that the crystallinity is a crucial factor to influence the colour.

The *a* vs. b** plots for **5a**–**6c**, and **7** (Table II) are shown in Fig. 11. **5a**–**5c** showing the similar colour result in the plots in the same area. On the other hand, **6a**–**6c**, and **7** bearing a 4-azophenyl-1-naphthol group feature the different *a** values. In particular, **6c** gives the largest *a** value. The results indicate that the difference in the crystallinity tends to be reflected by the *a** value.

CONCLUSION

The primary motif of the present study is to reproduce a flower palette system in a totally artificial system using saccharide-appended dye molecules. The obtained results indicate that the molecular packing mode of dye molecules can be

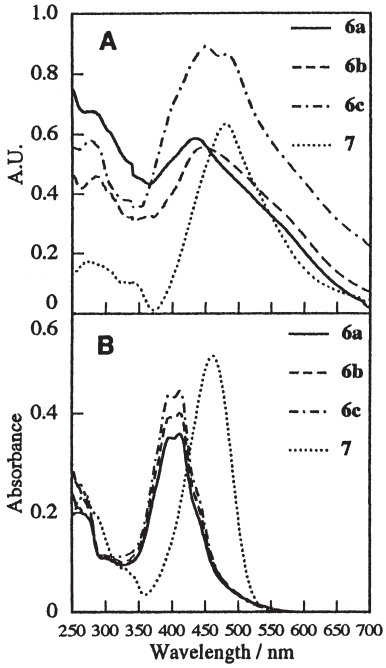

FIGURE 8 Absorption spectra of **6a**, **6b**, **6c**, and **7** (A) in solid (recrystallized from THF) and (B) in THF (2.00×10^{-5} mol dm^{-3}).

finely tuned by the appended saccharide moiety, which can be detected not only visually but also by absorption and XRD spectroscopic methods and a CIE *L*a*b** colourimetric system. Since dye molecules are functional molecules profoundly associated with redox potentials, fluorescence intensities, photosensitizers, digital memories, etc., we believe that these functions are also controllable using a saccharide library as a fine tuner.

EXPERIMENTAL SECTION

The compounds studied were prepared by diazonium coupling of aminophenyl glycosides with corresponding phenols and naphthols. The aminophenyl glycosides were prepared from nitrophenyl glycosides in a manner similar to the literature [25].

2-(4-β-D-Glucopyranosylphenylazo)-4-methylphenol (2a)

2-(4-β-D-Glucopyranosylphenylazo)-4-methylphenol (**2a**) was prepared according to the method of

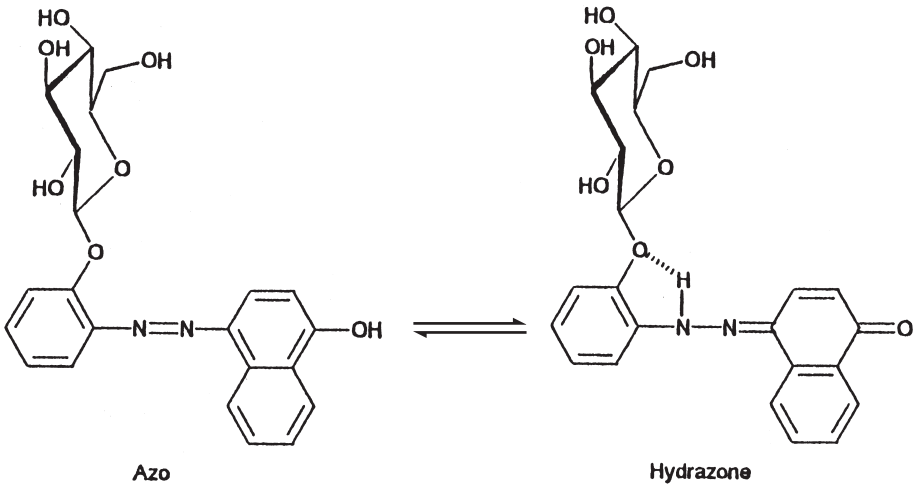

FIGURE 9 Influence of the 2′-phenyl-substituted saccharide on the azo-hydrazone tautomerism.

TABLE II Colour **5a-7**

	Colour	Solid state (crystallized from THF) λmax/nm[a]	Colour analysis[c] L*	a*	b*	Solution state (in THF) λmax/nm[b]
5a	red	420, 497, 550	31.8	45.0	82.3	420,460
5b	red	420, 494, 551	37.9	55.4	93.0	419, 460
5c	red	422, 493, 565	35.1	51.1	88.1	419, 462
6a	dark-red	433	19.8	17.3	11.1	397, 412
6b	dark-red	447	19.9	17.1	9.0	397, 411
6c	brown	450, 480	36.1	37.6	30.0	397, 412
7	red	481	31.1	5.3	20.1	461

[a] Measured by a KBr pellet method. [b] 5×10^{-5} mol dm^{-3} and $l = 1$ cm. [c] Colour analyses were performed according to the CIE L *a *b *colourimetric system. The values are averaged after three measurements.

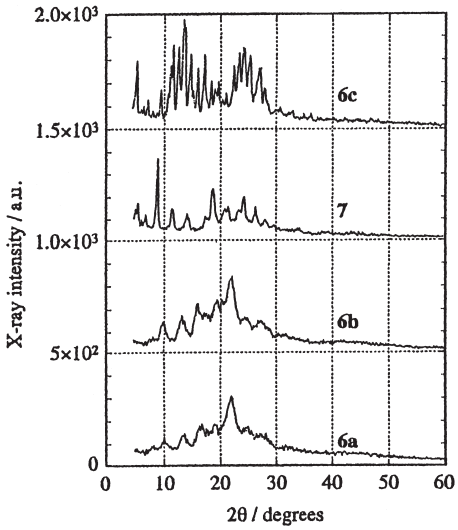

FIGURE 10 Powder XRD patterns for **6a**, **6b**, **6c**, and **7**.

Mcbroom *et al.* [26] with a minor modification. *p*-Aminophenyl-β-D-glucopyranoside (400 mg, 1.48 mmol) was dissolved in an icy aqueous solution of 0.1 mol dm^{-3} HCl (20 ml), and to this solution an icy aqueous solution of 0.05 mol dm^{-3} $NaNO_2$ (30 ml) was added dropwise with stirring. The mixture was cooled until the temperature of the stirred solution fell below 5°C. After stirring for 30 min, the solution of *p*-diazophenyl-β-D-glucopyranoside was added with stirring to an icy cold solution of *p*-cresol (320 mg, 2.96 mmol) and 1-propanol (30 ml) in 0.15 mol dm^{-3} NaCl (125 ml). The mixture was adjusted to pH 9 with 0.5 mol dm^{-3} NaOH and stirred for 6 h (the temperature was kept below 5°C). After neutralization with 0.1 mol dm^{-3} HCl, 1-propanol was removed by evaporation. The residue was extracted with ethyl acetate, and the organic solution was dried over anhydrous sodium sulfate and then evaporated *in vacuo*. The residue was purified by column chromatography on silica gel with ethyl acetate/methanol (10:1 v/v) as eluent. The product obtained was dried at 90°C for 4 h *in vacuo*. Compound **2a** was obtained as an dark yellow solid: Yield 50 %, mp 199–200°C; IR (KBr) ν_{max} 3377, 2880, 1600, 1584, 1504, 1437, 1242, 1076, 1042, 1017, 839, 754 cm^{-1}; ^{1}H NMR (DMSO-d$_6$) $\delta = 3.18–3.72$ (m, 6H), 4.61 (t, $J = 5.4$ Hz, 1H), 5.01–5.14 (m, 3H), 5.39 (d, $J = 4.5$ Hz, 1H), 6.94 (d, $J = 8.1$ Hz, 1H), 7.20 (d, $J = 8.7$ Hz, 2H), 7.54 (s, 1H), 7.95 (d, $J = 8.9$ Hz, 2H), 10.87 (s, 1H); m/z 391 [M]$^+$. Found: C, 57.98; H, 5.75; N, 7.05%. Calcd. for $C_{19}H_{22}N_2O_7$: C, 58.46; H, 5.68; N, 7.18%.

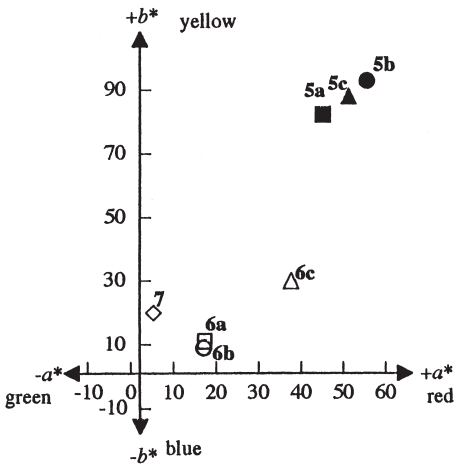

FIGURE 11 a^*–b^* plots for **5a**–**6c**, and **7**.

Releated compounds (**2b**, **3a**, **3b**, **4**, **5a**, **5b**, **6a**, **6b**, and **7**) were synthesized according to the similar method. We thus describe only their analytical data.

2-(4-β-D-Galactopyranosylphenylazo)-4-methylphenol (2b)

2-(4-β-D-Galactopyranosylphenylazo)-4-methylphenol (**2b**): yellow solid, yield 68%, mp 175–176°C; IR (KBr) ν_{max} 3365, 2912, 1599, 1497, 1437, 1279, 1242, 1143, 1082, 839, 787 cm^{-1}; ^{1}H NMR (DMSO-d$_6$) $\delta =$ 3.41–3.72 (m, 6H), 4.55 (d, $J = 4.8$ Hz, 1H), 4.69 (t, $J = 5.3$ Hz, 1H), 4.91 (d, $J = 5.7$ Hz, 1H), 4.98 (d, $J =$ 7.8 Hz, 1H), 5.24 (d, $J = 5.4$ Hz, 1H), 6.94 (d, $J =$ 8.4 Hz, 2H), 7.20 (d, $J = 8.1$ Hz, 3H), 7.54 (s, 1H), 7.97 (d, $J = 9.0$ Hz, 2H); m/z 391 [M]$^+$, Found: C, 58.00; H, 5.65; N, 7.15%. Calcd. for $C_{19}H_{22}N_2O_7$: C, 58.46; H, 5.68; N, 7.18%.

4-(4-β-D-Glucopyranosylphenylazo)phenol (3a)

4-(4-β-D-Glucopyranosylphenylazo)phenol (**3a**): yellow solid, yield 48%, mp 227–228°C; IR (KBr) ν_{max} 3256, 2878, 1601, 1499, 1412, 1238, 1076, 1047, 1009, 851, 754 cm^{-1}; ^{1}H NMR (DMSO-d$_6$) $\delta = 3.15–3.72$ (m, 6H), 4.59 (t, $J = 7.8$ Hz, 1H), 4.99 (d, $J = 7.2$ Hz, 1H), 5.06 (d, $J = 9.1$ Hz, 1H), 5.12 (d, $J = 4.5$ Hz, 1H), 5.34 (d, $J = 4.5$ Hz, 1H), 6.92 (d, $J = 6.9$ Hz, 2H), 7.18 (d, $J = 8.1$ Hz, 2H), 7.74–7.81 (m, 4H), 10.21 (s, 1H); m/z 376 [M]$^+$. Found: C, 54.49; H, 5.26; N, 7.30%. Calcd. for $C_{18}H_{20}N_2O_7$: C, 57.44; H, 5.36; N, 7.44%.

4-(4-β-D-Galactopyranosylphenylazo)phenol (3b)

4-(4-β-D-Galactopyranosylphenylazo)phenol (**3b**): pink solid, yield 32%, mp 231–232°C; IR (KBr) ν_{max} 3364, 2912, 1559, 1499, 1402, 1264, 1145, 1086, 1034, 849, 766 cm^{-1}; ^{1}H NMR (DMSO-d$_6$) $\delta = 3.31–3.72$ (m, 6H), 4.54 (d, $J = 4.5$ Hz, 1H), 4.68 (t, $J = 5.4$ Hz, 1H), 4.89–4.96 (m, 2H), 5.23 (d, $J = 5.1$ Hz, 1H), 6.92 (d, $J = 8.7$ Hz, 2H), 7.17 (d, $J = 9.0$ Hz, 2H), 7.74–7.81 (m, 4H), 10.21 (s, 1H); m/z 377 [M + H]$^+$, Found: C, 57.16; H, 5.39; N, 7.23%. Calcd. for $C_{18}H_{20}N_2O_7$: C, 57.44; H, 5.36; N, 7.44%.

4-(2-β-D-Glucopyranosylphenylazo)phenol (4)

4-(2-β-D-Glucopyranosylphenylazo)phenol (**4**): dark orange solid, yield 87%, mp 114–115°C; IR (KBr) υ_{max} 3310, 2882, 1592, 1507, 1486, 1281, 1230, 1148, 1075, 1013, 841, 754 cm^{-1}; ^1H NMR (DMSO-d_6) $\delta =$ 3.20–3.71 (m, 6H), 4.57 (t, $J = 7.8$ Hz, 1H), 5.04–5.14 (m, 3H), 5.28 (d, $J = 5.1$ Hz, 1H), 6.93 (d, $J =$ 6.9 Hz, 2H), 7.08 (t, $J = 8.0$ Hz, 1H), 7.73–7.53 (m, 3H), 7.82 (d, $J = 6.9$ Hz, 2H), 10.21 (s, 1H); m/z 376 $[M]^+$, Found: C, 57.32; H, 5.43; N, 7.37 %. Calcd. for $C_{18}H_{20}N_2O_7$: C, 57.44; H, 5.36; N, 7.44%.

1-(4-β-D-Glucopyranosylphenylazo)-2-naphthol (5a)

1-(4-β-D-Glucopyranosylphenylazo)-2-naphthol (**5a**): red solid, yield 51%, mp 220–221°C; IR (KBr) ν_{max} 3376, 2876, 1620, 1601, 1552, 1507, 1444, 1211, 1075, 1019, 829, 749 cm^{-1}; ^1H NMR (DMSO-d_6) $\delta =$ 3.21–3.68 (m, 6H), 4.52 (t, $J = 5.2$ Hz, 1H), 5.00 (d, $J = 5.0$ Hz, 1H), 5.03 (d, $J = 5.7$ Hz, 1H), 5.17 (d, $J =$ 6.3 Hz, 1H), 5.55 (d, $J = 3.5$ Hz, 1H), 7.13 (d, $J =$ 9.2 Hz, 1H) 7.31 (d, $J = 9.0$ Hz, 2H), 7.49 (t, $J =$ 7.1 Hz, 1H), 7.66 (d, $J = 7.1$ Hz, 1H), 7.89 (d, $J =$ 7.8 Hz, 1H), 7.97–8.02 (m, 3H), 8.71 (d, $J = 8.3$ Hz, 1H), m/z 427 $[M]^+$, Found: C, 61.57; H, 5.47; N, 6.40%. Calcd. for $C_{22}H_{22}N_2O_7$: C, 61.97; H, 5.20; N, 6.57%.

1-(4-β-D-Galactopyranosylphenylazo)-2-naphthol (5b)

1-(4-β-D-Galactopyranosylphenylazo)-2-naphthol (**5b**): red solid, yield 80%, mp 231–232°C; IR (KBr) ν_{max} 3357, 2870, 1619, 1603, 1559, 1507, 1397, 1242, 1148, 1088, 833, 749 cm^{-1}; ^1H NMR (DMSO-d_6) $\delta =$ 3.42–3.73 (m, 6H), 4.56 (d, $J = 4.5$ Hz, 1H), 4.70 (t, $J = 5.5$ Hz, 1H), 4.92 (d, $J = 5.7$ Hz, 1H), 4.97 (d, $J = 7.6$ Hz, 1H), 5.25 (d, $J = 5.2$ Hz, 1H), 7.11 (d, $J = 9.1$ Hz, 1H), 7.24 (d, $J = 8.7$ Hz, 2H), 7.47 (t, $J =$ 7.0 Hz, 1H), 7.64 (d, $J = 8.0$ Hz, 1H), 7.86 (d, $J =$ 8.7 Hz, 1H), 7.95–7.99 (m, 3H), 8.71 (d, $J = 8.4$ Hz, 1H), m/z 427 $[M]^+$, Found: C, 61.44; H, 5.32; N, 6.48%. Calcd. for $C_{22}H_{22}N_2O_7$: C, 61.97; H, 5.20; N, 6.57%.

1-(4-β-D-Glucopyranosylphenylazo)-4-naphthol (6a)

1-(4-β-D-Glucopyranosylphenylazo)-4-naphthol (**6a**): dark red solid, yield 77%, mp 190–191°C; IR (KBr) ν_{max} 3308, 2876, 1626, 1595, 1576, 1509, 1452, 1352, 1231, 1073, 1048, 1015, 833, 764 cm^{-1}; ^1H NMR (DMSO-d_6) $\delta = 3.20–3.74$ (m, 6H), 4.62 (t, $J = 5.2$ Hz, 1H), 5.00–5.14 (m, 3H), 5.40 (d, $J = 3.6$ Hz, 1H), 7.01 (d, $J = 8.5$ Hz, 1H), 7.23 (d, $J = 8.9$ Hz, 2H), 7.59 (t, $J = 7.1$ Hz, 1H), 7.70 (d, $J = 6.9$ Hz, 1H) 7.84 (d, $J =$ 6.9 Hz, 1H), 7.95 (d, $J = 8.9$ Hz, 2H), 8.23 (d, $J =$ 8.3 Hz, 1H), 8.89 (d, $J = 8.5$ Hz, 1H), 11.00 (s, 1H); m/z 427 $[M + H]^+$, Found: C, 62.12; H, 5.98; N, 6.31%. Calcd. for $C_{22}H_{22}N_2O_7$: C, 61.97; H, 5.20; N, 6.57%.

1-(4-β-D-Galactopyranosylphenylazo)-4-naphthol (6b)

1-(4-β-D-Galactopyranosylphenylazo)-4-naphthol (**6b**): dark red solid, yield 63%, mp 212–213°C; IR (KBr) ν_{max} 3362, 2870, 1620, 1590, 1576, 1509, 1449, 1350, 1240, 1076, 1055, 1017, 843, 766 cm^{-1}; ^1H NMR (DMSO-d_6) $\delta = 3.46–3.73$ (m, 6H), 4.55 (d, $J = 4.5$ Hz, 1H), 4.70 (t, $J = 5.4$ Hz, 1H), 4.91 (d, $J = 5.7$ Hz, 1H), 4.97 (d, $J = 7.5$ Hz, 1H), 5.25 (d, $J = 5.1$ Hz, 1H), 7.01 (d, $J = 8.4$ Hz, 1H) 7.23 (d, $J = 8.8$ Hz, 2H), 7.59 (t, $J = 7.3$ Hz, 1H), 7.69 (t, $J =$ 7.0 Hz, 1H), 7.84 (d, $J = 8.4$ Hz, 1H), 7.96 (d, $J = 8.8$ Hz, 2H), 8.23 (d, $J = 8.3$ Hz, 1H), 8.89 (d, $J = 8.5$ Hz, 1H), 11.03 (s, 1H); m/z 427 $[M + H]^+$, Found: C, 62.86; H, 5.60; N, 5.91%. Calcd. for $C_{22}H_{22}N_2O_7$: C, 61.97; H, 5.20; N, 6.57%.

1-(2-β-D-Glucopyranosylphenylazo)-4-naphthol (7)

1-(2-β-D-Glucopyranosylphenylazo)-4-naphthol (**7**): orange solid, yield 50%, mp 215–216°C; IR (KBr) ν_{max} 3281, 2882, 1624, 1597, 1538, 1458, 1417, 1318, 1269, 1213, 1073, 1088, 1047, 1015, 762 cm^{-1}; ^1H NMR ($CDCl_3 + CD_3COOD$) $\delta = 3.44–3.54$ (m, 5H), 3.78 (d, $J = 4.6$ Hz, 1H), 3.92 (d, $J = 10.7$ Hz, 1H), 6.74 (s, 1H), 7.12–7.23 (m, 2H), 7.37 (d, $J = 8.7$ Hz, 1H), 7.52 (t, $J = 7.7$ Hz, 1H), 7.70 (t, $J = 7.7$ Hz, 1H), 7.82 (d, $J =$ 9.3 Hz, 1H), 8.08–8.17 (m, 2H), 8.16 (br s, 1H); m/z 427 $[M + H]^+$, Found: C, 60.97; H, 5.28; N, 6.15%. Calcd. for $C_{22}H_{22}N_2O_7$: C, 61.97; H, 5.20; N, 6.57%.

2-(4-Methoxyphenylazo)-4-methylphenol (2c)

2-(4-Methoxyphenylazo)-4-methylphenol (**2c**): *p*-Anisidine (619 mg, 5.00 mmol) was dissolved in 15 ml of 1-propanol and 50 ml of water. Conc. HCl (0.75 ml) solution was added and the mixture was cooled until the temperature of the stirred solution fell below 5°C. Then, sodium nitrate (368 mg, 5.25 mmol) in 1.25 ml of water was added dropwise with stirring, and the mixtures was stirred for 30 min. The mixture was cooled until the temperature of the stirred solution fell below 5°C. The solution of *p*-cresol (681 mg, 6.30 mmol) in 1-propanol (20 ml) was added to this diazonium chloride solution. The mixture was adjusted to pH 9 with 0.5 mol dm^{-3} NaOH and stirred for 12 h (the temperature was kept below 5°C). After neutralization with 0.1 mol dm^{-3} HCl, 1-propanol was removed by evaporation. The residue was extracted with ethyl acetate, and the organic solution was dried over anhydrous sodium sulfate and then evaporated *in vacuo*. The residue was purified by column chromatography on silica gel with chloroform/ethyl acetate (10:1 v/v) as eluent. Compound **2c** dried at 90°C *in vacuo* was obtained as a brown

solid; yield 25%, mp 95.8–96.4°C; IR (KBr) ν_{max} 2945, 2840, 1603, 1585, 1496, 1437, 1246, 1159, 1107, 1036, 843, 804 cm^{-1}; ^1H NMR ($CDCl_3$) $\delta = 2.39$ (s, 3H), 3.91 (s, 3H), 6.92 (d, $J = 8.4$ Hz, 1H), 7.02 (d, $J = 9.0$ Hz, 2H), 7.14 (d, $J = 8.3$ Hz, 1H), 7.71 (s, 1H), 7.86 (d, $J = 9.0$ Hz, 2H), m/z 228 $[M]^+$. Found: C, 69.56; H, 5.82; N, 11.62%. Calcd. for $C_{14}H_{14}N_2O_2$: C, 69.41; H, 5.82; N, 11.56%.

Related compounds (**3c**, **5c**, and **6c**) were synthesized according to the similar method. We thus describe only their analytical data.

4-(4-Methoxyphenylazo)phenol (3c)

4-(4-Methoxyphenylazo)phenol (**3c**): blown solid, yield 50%, mp 145–146°C; IR (KBr) ν_{max} 3413, 1597, 1585, 1495, 1486, 1235, 1151, 1107, 1015, 843, 749 cm^{-1}; ^1H NMR ($CDCl_3$) $\delta = 3.90$ (s, 3H), 6.93 (d, $J = 8.8$ Hz, 2H), 7.02 (d, $J = 9.0$ Hz, 1H), 7.84 (d, $J = 8.8$ Hz, 2H), 7.89 (d, $J = 9.0$ Hz, 2H); Found: C, 68.35; H, 5.33; N, 12.18%. Calcd. for $C_{13}H_{12}N_2O_2$: C, 68.41; H, 5.30; N, 12.27%.

1-(4-Methoxyphenylazo)-2-naphthol (5c)

1-(4-Methoxyphenylazo)-2-naphthol (**5c**): dark red solid, yield 38%, mp 146–147°C; IR (KBr) ν_{max} 2956, 2838, 1601, 1584, 1504, 1433, 1302, 1248, 1159, 1028, 827, 754 cm^{-1}; ^1H NMR (DMSO-d_6) $\delta = 3.89$ (s, 3H), 7.15–7.19 (m, 3H), 7.49 (t, $J = 7.9$ Hz), 7.66 (t, $J = 7.3$ Hz, 1H), 7.89 (d, $J = 8.0$ Hz, 1H), 8.00–8.03 (m, 3H), 8.73 (d, $J = 8.4$Hz, 1H); m/z 278 $[M]^+$. Found: C, 73.38; H, 5.08; N, 10.16% Calcd. for $C_{17}H_{14}N_2O_2C$, 73.37; H, 5.07; N, 10.07%.

1-(4-Methoxyphenylazo)-4-naphthol (6c)

1-(4-Methoxyphenylazo)-4-naphthol (**6c**): dark brown solid, yield 48%, mp 181–182°C; IF (KBr) ν_{max} 3432, 2920, 2838, 1601, 1578, 1501, 1437, 1384, 1354, 1246, 1159, 1028, 839, 768 cm^{-1}; ^1H NMR (DMSO-d_6) $\delta = 3.87$ (s, 3H), 7.01 (d, $J = 8.4$ Hz, 1H), 7.14 (d, $J = 7.7$ Hz, 2H), 7.56–7.72 (m, 2H), 7.82 (d, $J = 8.4$ Hz, 2H), 7.96 (t, $J = 9.0$ Hz, 1H), 8.23 (d, $J = 8.1$ Hz, 1H), 8.87 (d, $J = 9.3$ Hz, 1H); m/z 278 $[M]^+$. Found: C, 73.37; H, 5.14; N, 9.72%. Calcd. for $C_{17}H_{14}N_2O_2$: C, 73.37; H, 5.07; N, 10.07%.

MISCELLANEOUS

Column chromatography was performed on silica gel (Wako Gel C-300). Melting points were determined on a Micro Melting Point Apparatus Yanaco MP-500D. UV spectra for solutions and solids (KBr pellet) were measured at 20°C using a JASCO V-570 spectrophotometer. ^1H NMR spectra were measured on a Bruker ARX 300 apparatus. IR spectra were obtained in KBr pellets using a Shimadzu FT-IR 8100 spectrometer. MS spectra were obtained by a Hitachi M-2500 mass spectrometer. The colourimetric measurements were carried out with a tristimulus colourmeter (SC-2-CH, Suga Test Instruments). XRD was measured with a DIP2000 imaging plate system (Mac Science Co., Ltd) and a M18XHF-SRA rotating anode X-ray generator or a JEOL X-ray diffractmeter JDX-8020.

Acknowledgements

We are grateful to Professor T. Kajiyama and Dr S. Sasaki (Faculty of Applied Chemistry, Graduate School of Engineering, Kyushu University) where we carried out X-ray measurements.

References

[1] Haslam, E. (1993), *Chem. Br.*, 875.
[2] Misumi, S. (1993), *Kagaku To Kogyo (Chem. Ind.)* **46**, 756.
[3] Goto, T. and Kondo, T. (1991), *Angew. Chem. Int. Ed. Engl.* **30**, 17.
[4] Mohler, L.K. and Czarnic, A.W. (1993), *J. Am. Chem. Soc.* **115**, 2998.
[5] Tsukagoshi, K. and Shinkai, S. (1991), *J. Org. Chem.* **56**, 4089.
[6] Shiomi, Y., Saisho, M., Tsukagoshi, K. and Shinkai, S. (1993), *J. Chem. Soc., Perkin Trans.* **1**, 2111.
[7] Shinkai, S., Tsukagoshi, K., Ishikawa, Y. and Kunitake, T. (1991), *J. Chem. Soc., Chem. Commun.*, 1040.
[8] Ludwig, R., Ariga, K. and Shinkai, S. (1993), *Chem. Lett.*, 1413.
[9] Kondo, K., Shiomi, Y., Saisho, M., Harada, T. and Shinkai, S. (1992), *Tetrahedron* **48**, 8239.
[10] James, T.D., Harada, T. and Shinkai, S. (1993), *J. Chem. Soc., Chem. Commun.*, 857.
[11] James, T.D., Sandanayake, K.R.A.S. and Shinkai, S. (1996), *Angew. Chem. Int. Ed.* **35**, 1910.
[12] James, T.D., Linnane, P. and Shinkai, S. (1996), *Chem. Commun. (Feature Article).*, 281.
[13] Sandanayake, K.R.A.S. and Shinkai, S. (1994), *Chem. Commun.*, 1083.
[14] Nagasaki, T., Shinmori, H. and Shinkai, S. (1994), *Tetrahedron Lett.* **35**, 2201.
[15] Shinmori, H., Takeuchi, M. and Shinkai, S. (1995), *Tetrahedron* **51**, 1893.
[16] Koumoto, K., Takeuchi, M. and Shinkai, S. (1998), *Supramol. Chem.* **9**, 203.
[17] Davis, C.J., Lewis, P.T., McCarroll, M.E., Read, M.W., Cueto, R. and Stongin, R.M. (1999), *Org. Lett.* **1**, 331.
[18] Lewis, P.T., Davis, C.L., Cabell, L.A., He, M., Read, M.W., McCarroll, M.E. and Strongin, R.M. (2000), *Org. Lett.* **2**, 589.
[19] Ward, C.J., Patel, P., Ashton, P.R. and James, T.D. (2000), *Chem. Commun.*, 229.
[20] Wyszecki, G. and Stiles, W.S. (1982) Colour Science, 2nd Ed. (Wiley, New York).
[21] Gabor, G., Frei, Y., Gegiou, D., Kaganowitch, M. and Fischer, E. (1967), *Isr. J. Chem.* **5**, 193.
[22] Schreiber, J., Socha, J. and Rothschein, K. (1970), *Collect. Czech. Chent. Commun.* **35**, 857.
[23] Kishimoto, S., Kitahara, S., Manabe, O. and Hiyama, H. (1978), *J. Org. Chem.* **43**, 3882.
[24] Kelemen, J. (1981), *Dye Pigm.* **2**, 73.
[25] Amaike, M., Kobayashi, H. and Shinkai, S. (2000), *Bull. Chem. Soc. Jpn* **73**, 2553.
[26] Mcbroom, C.R., Samanen, C.H. and Goldstein, I.J. (1972), *Methods Enzymol.* **28**, 212.